NATIONAL ADVISORY COMMITTEE FOR AERONAUTICS

TECHNICAL NOTE 2894

CALCULATIONS OF UPWASH IN THE REGION ABOVE OR

BELOW THE WING-CHORD PLANES OF SWEPT-BACK

WING-FUSELAGE-NACELLE COMBINATIONS

By Vernon L. Rogallo and John L. McCloud, III

Ames Aeronautical Laboratory
Moffett Field, Calif.

NACA

Washington

February 1953

NATIONAL ADVISORY COMMITTEE FOR AERONAUTICS

TECHNICAL NOTE 2894

CALCULATIONS OF UPWASH IN THE REGION ABOVE OR

BELOW THE WING-CHORD PLANES OF SWEPT-BACK

WING-FUSELAGE-NACELLE COMBINATIONS

By Vernon L. Rogallo and John L. McCloud, III

SUMMARY

A procedure has been developed for predicting the upwash compo-
nents of the upflow angles in the region above or below the wing-chord
planes of swept-back wing-fuselage-nacelle combinations. This procedure
entails modifications to the methods given in NACA TN's 2528 and 2795,
for predicting induced upwash angles.

Comparisons of predicted and measured upflow angles are shown for
six semispan models with 40° swept-back wings. The models differ mainly
in nacelle location (spanwise, chordwise, and vertical relative to the
wing). For all models, the agreement between the measured and predicted
upflow angles was found to be good for all points along the horizontal
center line of the propeller disks.

The accuracy of the upflow angles obtained by this procedure is
considered satisfactory for use in estimating propeller vibratory
stresses.

INTRODUCTION

It has been shown in reference 1 that the oscillating aerodynamic
loadings on propellers, which contribute to the vibratory stresses, are
directly dependent upon the upflow angles[1] at the horizontal center line
of the propeller disk. A method for predicting the upwash angle contri-
butions to the upflow angles, including the effects of wing, nacelle,
and fuselage, for a twin-engine airplane having an unswept wing is
given in reference 2. The method of reference 2 has been extended in
reference 3 to show the effects of wing sweep on the upwash.

[1]Angle between the thrust axis and the direction of local flow measured
in a plane parallel to the model vertical plane of symmetry.

The methods as developed in references 2 and 3 have the following limitations: The fuselage induction effects are limited to the extended horizontal plane of symmetry; and the wing upwash of reference 3 is only applicable in the region of the extended wing-chord plane.

It is the purpose of this report to present modifications to the existing methods to remove the above-mentioned limitations, and to present experimental evidence by which to assess the accuracy of the modified methods.

NOTATION

A   total upflow angle $(\alpha_w + \epsilon_w + \epsilon_n + \epsilon_b + \gamma)$

b   wing span

c   wing chord at inboard nacelle

C_L wing lift coefficient $\left(\dfrac{\text{lift}}{qS}\right)$

q   dynamic pressure

R   radius of body

S   wing area

U   longitudinal component of free-stream velocity $(V_o \cos \alpha_b)$

ΔU increase in longitudinal velocity

V_o free-stream velocity

W   cross component of free-stream velocity $(V_o \sin \alpha_b)$

ΔW increase in cross velocity

i_w angle of wing with respect to fuselage center line[2]

x_w longitudinal distance ahead of wing quarter-chord line

y_b lateral distance from body center line

y_w lateral distance from longitudinal center line of wing

---

[2]Measured in a plane parallel to the model plane of symmetry.

z_b vertical distance from body center line

z_w vertical distance from wing-chord plane

α_b effective angle of attack of the longitudinal axis of a body[2]
       $(\alpha_w + \epsilon_w - i_w)$

α_w wing angle of attack[2] with respect to free-stream direction

β compressibility parameter $[\sqrt{(1-M^2)}\,]$

γ nacelle-longitudinal-axis inclination as measured from the local
       chord[2] (negative below wing-chord line)

ϵ angle of upwash[2] measured from free-stream direction

ζ vertical coordinate $\left(\dfrac{z_w}{b/2}\right)$, semispans

η lateral coordinate $\left(\dfrac{y_w}{b/2}\right)$, semispans

τ longitudinal coordinate $\left(\dfrac{x_w}{b/2}\right)$, semispans

Λ sweep angle of quarter-chord line, positive for sweepback

Subscripts

w   wing

n   nacelle

b   body

---

[2]See footnote 2, p. 2.

PROCEDURE

The basic procedure used in computing the upwash in this report is
the same as that used in existing methods of references 2 and 3; namely,
the total upwash angle at a point is assumed equal to the sum of the
upwash angles induced by the wing, nacelle, and fuselage. The wing
upwash is due to the wing lift and is calculated using lifting—line or
lifting—surface theory and the fuselage and nacelle upwash are calcu-
lated from potential flow equations for an infinite cylinder and semi-
infinite body, respectively.

Wing—Induced Upwash

Although the lifting—line theory used in reference 2 is applicable
in regions above or below the wing—chord plane, it is not directly
applicable to swept wings. The simplified lifting—surface method of
reference 3 enables calculation of the upwash ahead of wings of arbi-
trary plan form, but only in the wing—chord plane. Thus to determine
the upwash in regions other than the wing—chord plane for wings of
arbitrary plan form, it is necessary to extend or modify the existing
methods.

For simplicity, the lifting—surface method of reference 3 has been
modified. The modification is based on the assumption that the vertical
variation of upwash from a wing is similar to the vertical variation of
upwash from a horseshoe vortex. For low Mach numbers, the bound vortex
has the same sweep as the wing quarter—chord line, and lies in the wing-
chord plane.[3] For a value of η and τ/β, the vertical variation of
upwash due to the horseshoe vortex is readily found from the following
equation which corresponds to equation (34) of reference 4.

---

[3] For high Mach numbers, the horseshoe vortex should have a sweep
angle Λ_β given by $\tan \Lambda_\beta = (\tan \Lambda)/\beta$ in accordance with the
Prandtl—Glauert rule.

$$\frac{\epsilon}{\beta C_L} = \frac{1}{4\pi\beta b^2/s} \left\{ -\left[\frac{1-\eta}{\zeta^2+(1-\eta)^2}\right] - \left[\frac{1+\eta}{\zeta^2+(1+\eta)^2}\right] + \right.$$

$$\frac{\left[\dfrac{\tau/\beta}{(\tau/\beta)^2+\zeta^2/\cos^2\Lambda_\beta}\right]\left[\left(\tau/\beta\,\tan\Lambda_\beta + \dfrac{1-\eta}{\cos^2\Lambda_\beta}\right)\right] + \left[\dfrac{1-\eta}{\zeta^2+(1-\eta)^2}\right]\left\{\left[\tau/\beta+(1-\eta)\,\tan\Lambda_\beta\right]\right\}}{\sqrt{[\tau/\beta + (1-\eta)\,\tan\Lambda_\beta]^2 + (1-\eta)^2 + \zeta^2}} -$$

$$\frac{\left[\dfrac{2\eta\,\tan\Lambda_\beta-\tau/\beta}{(2\eta\,\tan\Lambda_\beta-\tau/\beta)^2+\zeta^2/\cos^2\Lambda_\beta}\right]\left[\left(\tau/\beta\,\tan\Lambda_\beta + \dfrac{1-\eta}{\cos^2\Lambda_\beta}\right) + 2\eta\right] - \left[\dfrac{1+\eta}{\zeta^2+(1+\eta)^2}\right]\left\{\left[\tau/\beta+(1-\eta)\,\tan\Lambda_\beta\right]\right\}}{\sqrt{[\tau/\beta + (1-\eta)\,\tan\Lambda_\beta]^2 + (1+\eta)^2 + \zeta^2}} -$$
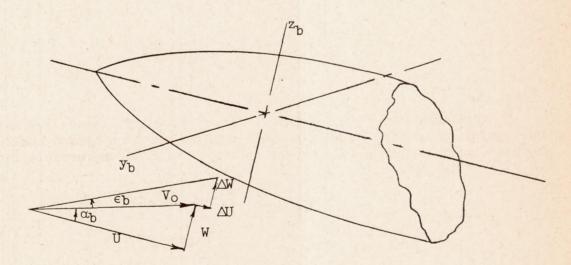
$$\left.\frac{\left[\dfrac{\tau/\beta}{(\tau/\beta)^2+\zeta^2/\cos^2\Lambda_\beta}\right]\left(\tau/\beta\,\tan\Lambda_\beta - \dfrac{\eta}{\cos^2\Lambda_\beta}\right) - \left[\dfrac{2\eta\,\tan\Lambda_\beta-\tau/\beta}{(2\eta\,\tan\Lambda_\beta-\tau/\beta)^2+\zeta^2/\cos^2\Lambda_\beta}\right]\left[\left(\tau/\beta\,\tan\Lambda_\beta - \dfrac{\eta}{\cos^2\Lambda_\beta}\right) + 2\eta\right]}{\sqrt{(\eta\,\tan\Lambda_\beta - \tau/\beta)^2 + \eta^2 + \zeta^2}} \right\}$$

If the upwash at a point above or below the wing–chord plane is expressed as a percentage of the upwash in the wing–chord plane, this percentage may be used to determine the wing upwash at a corresponding η, τ/β, and distance above or below the wing–chord plane. To show a typical example, the upwash expressed in this manner is presented in figure 1 for a $40°$ swept–back horseshoe vortex system.

Fuselage–Induced Upwash

In the previous applications of the methods of references 2 and 3, the horizontal center lines of the propeller planes were coincident with the median plane of the fuselage. In order to calculate upwash at the horizontal center line of propeller planes which are not coincident with the fuselage median plane, the method used in references 2 and 3 must be extended. The velocity components (in a vertical plane parallel to the body longitudinal axis) of the flow about an inclined body are shown in the following sketch.

From the geometry of the velocity components

$$\tan\left(\alpha_b + \epsilon_b\right) = \frac{W + \Delta W}{U + \Delta U} = \frac{1 + \frac{\Delta W}{W}}{\frac{U}{W} + \frac{\Delta U}{W}} = \frac{W}{U}\left(\frac{1 + \frac{\Delta W}{W}}{1 + \frac{\Delta U}{U}}\right) \tag{1}$$

therefore, since $W/U = \tan\alpha_b$,

$$\frac{\tan\left(\alpha_b + \epsilon_b\right)}{\tan\alpha_b} = \frac{1 + \frac{\Delta W}{W}}{1 + \frac{\Delta U}{U}} \tag{2}$$

which for small angles (α_b and ϵ_b) may be written

$$\frac{\alpha_b + \epsilon_b}{\alpha_b} = 1 + \frac{\epsilon_b}{\alpha_b} \cong \frac{1 + \frac{\Delta W}{W}}{1 + \frac{\Delta U}{U}} \tag{3}$$

If ΔW and ΔU can be found for any point in space, ϵ_b is known for that point. Although it is difficult to find these quantities for a finite body, they are readily obtained for the infinite cylinder in incompressible flow.

For a fuselage which has a large fineness ratio and extends well forward of the propeller plane (at least three maximum mean diameters), it may be assumed that the fuselage can be represented by an infinite cylinder equal in diameter to that of the cross section of the fuselage in the extended propeller plane (see reference 2).[4] In the case of an infinite cylinder, ΔU is equal to zero, hence equation 3 becomes

$$1 + \frac{\epsilon_b}{\alpha_b} \cong 1 + \frac{\Delta W}{W} \quad \text{or} \quad \frac{\epsilon_b}{\alpha_b} \cong \frac{\Delta W}{W} \tag{4}$$

To determine the increase in cross-flow velocity, the well-known source-sink or doublet equations found in most texts on hydrodynamics are used. For an infinite circular cylinder in an incompressible flow

$$\frac{\Delta W}{W} = \frac{\left(\frac{y_b}{R}\right)^2 - \left(\frac{z_b}{R}\right)^2}{\left[\left(\frac{y_b}{R}\right)^2 + \left(\frac{z_b}{R}\right)^2\right]^2} \cong \frac{\epsilon_b}{\alpha_b} \tag{5}$$

The lateral distribution of ϵ_b/α_b at constant distances above or below the median plane of an infinite circular cylinder is presented in figure 2.

---

[4] The validity of this assumption has not been checked for the case of compressible flow.

RESULTS

To provide experimental data for evaluation of the modified methods, surveys were made of the upflow angles at the horizontal center line of the propeller disks for six semispan models with 40° swept-back wings. The surveys were made in the Ames 40- by 80-foot wind tunnel at a Mach number of 0.13. One of the models is shown mounted in the wind tunnel in figure 3. All six models are shown in figure 4. The survey rake shown in figure 3 consisted of six directional-pitot-static tubes mounted at various intervals along a steel tube. The method of reference 3, together with the modifications included herein, has been used to predict the upwash angles, which are combined with the geometric angles to obtain the upflow angles for the six models. Comparison of the measured and predicted upflow angles at several locations along the horizontal center line of each propeller disk is shown in figure 5. Upflow angles are shown for angles of attack of -4°, 0°, 4°, 8°, and 10°. Although not evident from figure 5, the agreement between the measured and predicted upflow angles was found to be of the same order at various points along the horizontal center line of the propeller disks and for the different nacelle locations at a given angle of attack.

CONCLUDING REMARKS

A procedure for predicting the upwash component of the upflow angles in the region above or below the wing-chord planes of swept-back wing-fuselage-nacelle combinations has been developed and evaluated.

The accuracy of the upflow angles obtained by this procedure is considered satisfactory for use in estimating propeller vibratory stresses.

Ames Aeronautical Laboratory
    National Advisory Committee for Aeronautics
        Moffett Field, Calif., Nov. 14, 1952

REFERENCES

1. Roberts, John C., and Yaggy, Paul F.: A Survey of the Flow at the
    Plane of the Propeller of a Twin-Engine Airplane. NACA TN 2192,
    1950.

2. Yaggy, Paul F.: A Method for Predicting the Upwash Angles Induced
    at the Propeller Plane of a Combination of Bodies With an Unswept
    Wing. NACA TN 2528, 1951.

3. Rogallo, Vernon L.: Effects of Wing Sweep on the Upwash at the Propeller Planes of Multiengine Airplanes. NACA TN 2795, 1952.

4. Spreiter, John R., and Sacks, Alvin H.: The Rolling Up of the Trailing Vortex Sheet and Its Effect on the Downwash Behind Wings. Jour. Aero. Sci., vol. 18, no. 1, Jan. 1951.
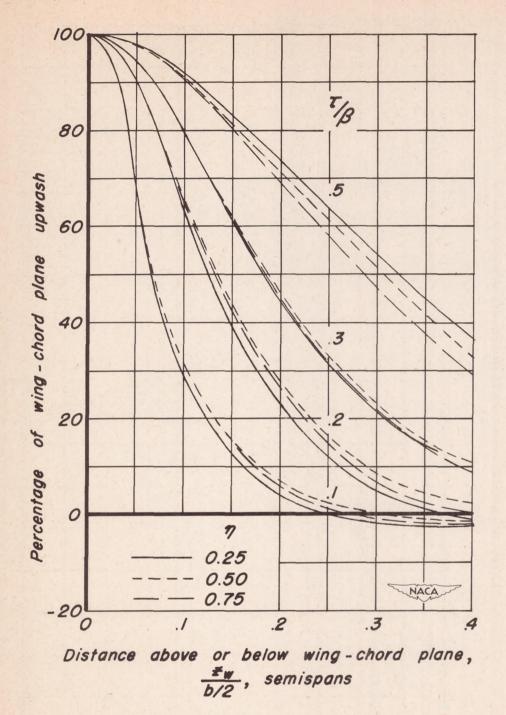
Figure 1.- Variation of upwash of a 40° swept-
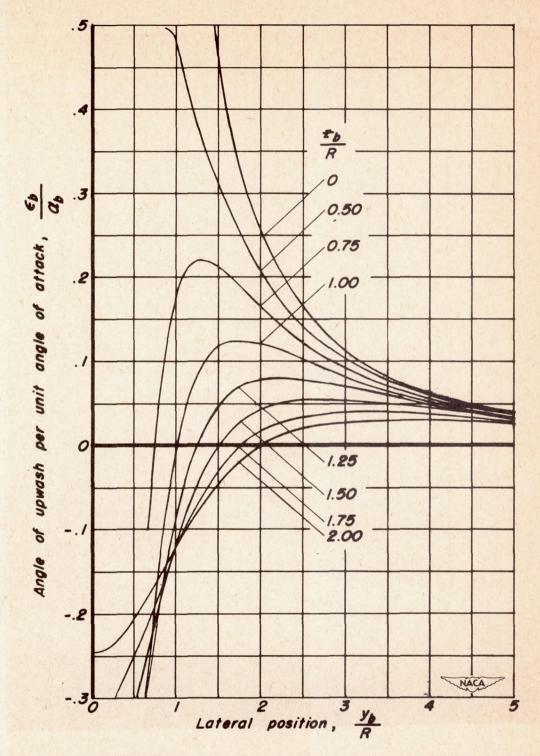back horseshoe vortex with vertical position.

Figure 2.- The upwash of an infinite cylinder in a transverse plane.

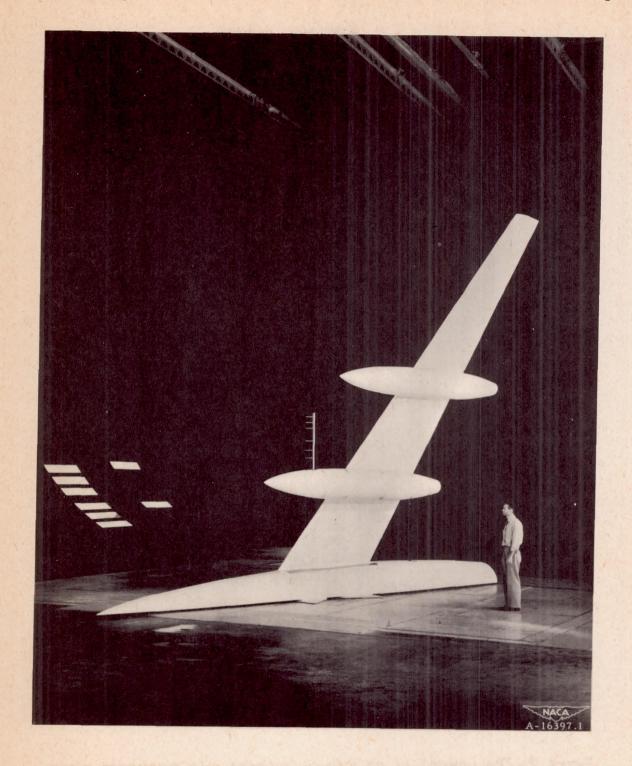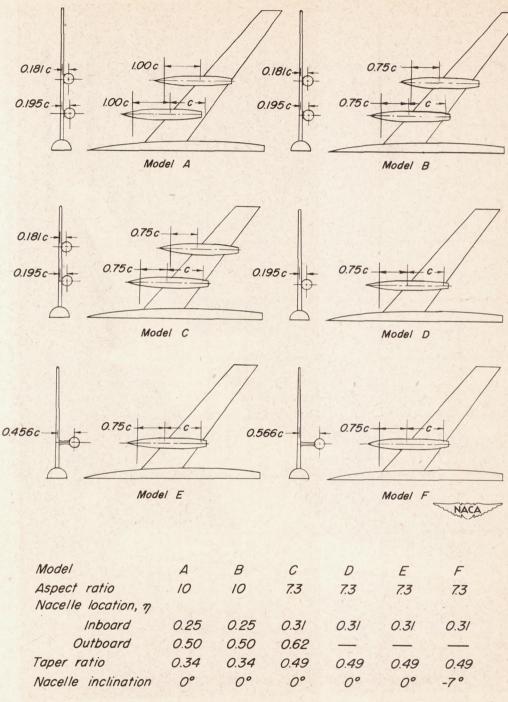Figure 3.— Model B mounted in the 40— by 80—foot wind tunnel.

Figure 4. — Semispan models. Λ, 40°.

Model	A	B	C	D	E	F
Aspect ratio	10	10	7.3	7.3	7.3	7.3
Nacelle location, η						
Inboard	0.25	0.25	0.31	0.31	0.31	0.31
Outboard	0.50	0.50	0.62	—	—	—
Taper ratio	0.34	0.34	0.49	0.49	0.49	0.49
Nacelle inclination	0°	0°	0°	0°	0°	-7°

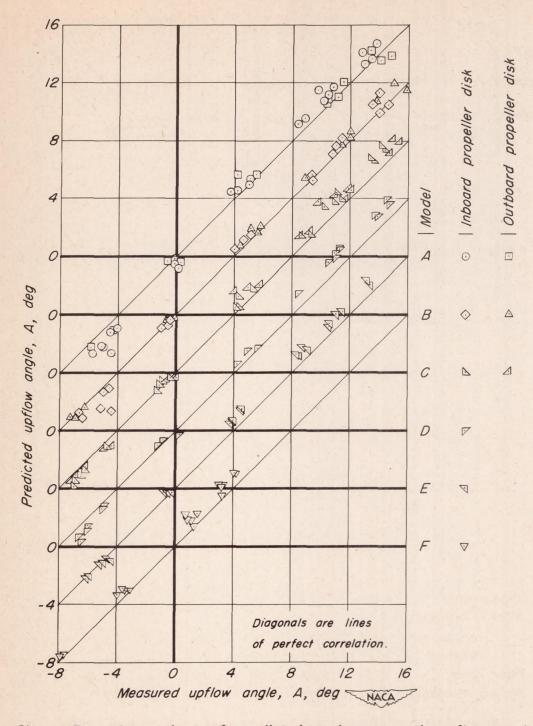Note: Extent of survey from nacelle center line, 0.19c to 0.61c.

Figure 5.— Comparison of predicted and measured upflow angles for six semispan models at several angles of attack.